Journal of Nano Research
ISSN: 1661-9897, Vol. 74, pp 69-82
doi:10.4028/p-41b175

Submitted: 2022-02-04
Revised: 2022-05-18
Accepted: 2022-05-23
Online: 2022-07-12

Study and Comparison of Different Routes to Synthesize Reduced Graphene Oxide

Rodolfo Fernández-Martínez[1,a*], Mª Belén Gómez-Mancebo[1,b], Laura J. Bonales[2,c], César Maffiotte[1,d], Alberto J. Quejido[1,d] and Isabel Rucandio[1,e]

[1]Department of Technology. Centro de Investigaciones Energéticas, Medioambientales y Tecnológicas (CIEMAT), Madrid, 28040, Spain.

[2] Astrobiology Center (CAB-CSIC-INTA), Torrejón de Ardoz (Madrid), 28850, Spain

[a*]rodolfo.fernandez@ciemat.es, [b]mariabelen.gomez@ciemat.es, [c]ljbonales@cab.inta-csic.es, [d]cesar.maffiotte@ciemat.es, [e]alberto.quejido@ciemat.es, [f]isabel.rucandio@ciemat.es

Keywords: Graphene oxide, reduced graphene oxide, Tour method, Hummers method, chemical exfoliation

Abstract. The feasibility of graphene oxide (GO) obtained by both Hummers and Tour method to prepare reduced graphene oxide (rGO) as well as chemically reduction under different experimental conditions were evaluated with the objective of establishing the key items that should be considered when performing the synthesis of GO and rGO. This key items can be supportive to select the most feasible methodology to synthesize GO and rGO depending on the future application. Reduced graphene oxide was prepared by combining chemical and solvothermal as well as combined reduction adding a final thermal annealing step. Obtained GO and rGO were characterized by XRD, Raman spectroscopy, XPS and BET analysis. A higher oxidation degree was achieved for samples from Tour method than those oxidized by Hummers method. On the contrary, lower oxidation degree from Hummers graphene oxide (GO-H) facilitates the subsequent reduction process, leading to a higher reduced rGO. Hence, rGO samples obtained from the Hummers method in the different reduction treatments presented higher C/O atomic ratios than the corresponding Tour method. In addition, the combination of a solvothermal treatment and chemical reduction, including a final annealing stage, increases significantly the value of the C/O ratio as well as it contributes to decrease the defect density and the restoration of π-conjugated structure. Besides, rGO samples obtained from Tour method presented higher SSA and pore volume than those samples obtained from Hummers method. Results from this study suggest the suitability of Tour graphene oxide (GO-T) for chemical functionalization which is very useful for several applications. In addition, GO and rGO coming from Tour method are more appropriate to applications in which high surface area is required. Taking into account the vast possible applications for chemically-exfoliated graphene the findings of this study could help to select the best method for oxidising graphite depending on the intended application.

Introduction

Graphene is a material with worldwide popularity due to its unique features such as electrical conductivity, mechanical strength, thermal conductivity, optical transparency and high specific surface [1-4]. There are many ways to synthetize this compound and graphene related materials. One of the most promising approaches to obtain reduced graphene oxide (rGO) with low cost and high yield is via chemical oxidation from graphite, exfoliation to give graphene oxide (GO) and subsequent reduction. Moreover, rGO obtained by the oxidation-exfoliation-reduction route constitutes the most important procedure to achieve the scalable production of graphene materials, which is crucial for applications such as composites, electronics, energy storage, catalytic or biosensor [5-8]. Regarding oxidation, graphite oxide exhibits an identical layered structure to graphite, but it contains a large quantity of oxygen-containing groups, which results in an increase in the interlayer spacing and makes the atomic-thick layers hydrophilic as well [9]. Therefore,

graphite oxide layers can be easily exfoliated in water by mild ultrasonication. Moreover, the presence of oxygen functionalities provides anchoring points for subsequent chemical modification which are necessary to be functionalized with metals and organic molecules and for doping with heteroatoms [10]. One of the most applied oxidation methods was developed by Hummers and Offeman [11] in which $NaNO_3$ and $KMnO_4$ dissolved in concentrated H_2SO_4 are used to oxidize graphite in a three-step process with time and temperature control within a few hours. Hummers method has been widely accepted to afford GO, but it presents several flaws, mainly related with toxic gases generation (NO_2, N_2O_4) and relatively low yield. Also, a variation of this method, commonly named as modified Hummers method, has been widely applied. This last method reduces the reaction cycle and it increases the reaction efficiency [12]. Another method to produce GO was introduced by Marcano et al. [13] by increasing the amount of $KMnO_4$ and introducing H_3PO_4 instead of $NaNO_3$. This, so-called Tour method, provides a greater amount of hydrophilic oxidized graphene material compared to Hummers and improved Hummers methods. Obtained GO materials can be applied to a great variety of applications and, also, constitute the intermediate materials for the manufacture of reduced graphene oxide (rGO), a homogeneous material with structural defects, resulting from the partial elimination of oxygen functional groups decorated on GO [14].

After graphite oxidation and exfoliation to produce graphene oxide (GO) the reduction of GO is performed to restore or simulating the pristine graphene structure. The reduction of GO leads to loss of functional groups on its surface, resulting in increased hydrophobicity. However, it is difficult to produce rGO due to its tendency to easily agglomerate in solvents. Therefore, to overcome this problem various research efforts have been performed. Different strategies can be used to obtain rGO: chemical reduction, this means, by employing chemical reagents like hydrazine, sodium hydroxide, alcohols, vitamin C, and sodium borohydride [15-18]. Hydrazine is one of the most widely used reducing agents, but it is also highly toxic and potentially explosive [19], so its use should be avoided in the large-scale implementation. Some authors prefer using L-ascorbic acid, vitamin C, which is a potent reducing agent as well as a green alternative for conventional reducing agents of GO [20,21]. Thermal or photothermal treatment is other approach employed to obtain rGOs materials. These ways are easier and faster than chemical via, and also are environmentally friendly, being used in several applications [22-24]. Another well-established reduction method is the solvothermal reduction that combines simplicity and effectiveness [25]. In this method, graphene oxide suspensions in a variety of solvents are heated in a sealed container at high temperature either in an autoclave or in an open system. However, for both routes the resulting reduced graphene oxide (rGO) still contains a considerable amount of heteroatoms and defects, and thus further thermal treatment at higher temperature is required for removing them. Typical thermal treatment includes annealing [26].

On top of that, recent studies revealed that the multistep reduction strategies, resulting from the combination of reduction methods lead to an improvement in the removal of oxygen functional groups [27] and can provide highly reduced graphene oxide with superior characteristics in terms of conductivity and chemical and thermal stability.

Since rGO properties that determine its applicability such as specific surface area, conductivity and oxygen functionalities abundance are dependent of the reduction process, controlled synthesis is essential to obtain suitable rGO for a specific application. Taking into account the advantages offered by multiphase reduction methods to modulate the reduction degree of GO as well as other properties such as specific surface and pore size, herein we reported the results obtained from the application of several reduction strategies over GO obtained by both the Hummers and Tour methods. In order to check the effect that can be produced on the properties of the synthesized rGOs by the combination of two or even three different reductions, two reducing routes consisting on multiphase reduction methods are evaluated: (1) a combination of chemical and solvothermal method and (2) a combination of chemical, solvothermal and final thermal annealing at different temperatures.

The efficiency will be evaluated thoroughly by the comparison of structural, morphology and chemical properties of each prepared materials.

Materials and Methods

Three different reduction methods were employed to produce rGO materials. Chemical method was evaluated alone and in combination with solvothermal and thermal treatment (Table 1). These multiphase treatments were applied to maximize the removing of oxygen functional groups in graphene oxide.

Materials. Graphite powder (200 mesh, 99,9995%) was purchased from United Carbon Products (MI, USA). Concentrated sulfuric acid (H_2SO_4, 98% w/w), sodium nitrate ($NaNO_3$), potassium permanganate ($KMnO_4$), hydrogen peroxide (H_2O_2, 30% V/V), phosphoric acid (H_3PO_4, 85% w/w) and Ascorbic Acid were of analytical grade and were purchased from Merck (Darmstadt, Germany). Ultrapure water (Resistivity ≥ 18.2 MΩ.cm) from a Milli-Q system (Millipore Bedford, MA, USA) was used throughout.

Synthesis of graphite oxide. GrO was synthesized from graphite powder by:

a) Modified Hummers method. To obtain graphite oxide by Hummers method (GrO-H), 3 g of graphite powder and 1.5 g of $NaNO_3$ were mixed with 70 mL of concentrated H_2SO_4 and placed in an ice bath. The mixture was stirred in a plate and 9 g of $KMnO_4$ were slowly added in portions to keep the reaction temperature below 15 ˚C. This mixture was stirred for 1 h and then the ice bath was removed, and its temperature increased up to 35 ± 5 ˚C by applying external heating keeping the stirring for another 2 h. Subsequently, 230 mL of ultrapure water were added producing a highly exothermic reaction. The temperature was kept below 70 ºC during the addition of water. Then, external heating was applied to reach and maintain the reaction temperature at 90 ± 0.5 ºC for 0.5 h. Shortly, 50 mL of H_2O_2 and 200 mL ultrapure water were added resulting in a brilliant yellow color along with bubbling. The obtained yellow-brown suspension was then cooled to room temperature, allowed to settle overnight and clear supernatant decanted. The remaining mixture was transferred to centrifuge tubes and washed with 150 mL ultrapure water for five times after separation of supernatants by centrifugation (10000 rpm, 1 h). Finally, the obtained solid was dried under vacuum at 40 ˚C for 2 days.

b) Tour method. Graphite oxide from Tour method (GrO-T) was prepared by mixing 3 g of graphite powder with 18 g of $KMnO_4$. 400 mL of a mixture of H_2SO_4/H_3PO_4 (9:1 volume ratio) were added. Then, the mixture was stirred in a stirring-hot plate at 50 ºC for 16 h changing its color from dark purplish to dark brown. 400 mL of ice ultrapure water and 10 mL of 30% H_2O_2 were added to finish oxidation reaction resulting in a bright yellow suspension. Acidic supernatant was decanted and supernatant removed. The obtained GrO-T was washed and dried similarly to GrO-H.

Reduction of graphene oxide. For each experiment 0.15 g of as-prepared dried GrO powder were suspended in 300 mL of ultrapure water and ultrasonicated for 200 minutes to exfoliate until formation of homogenous dispersions of 0.5 mg.mL-1 of graphene oxide (GO). Then, three different treatments have been applied to reduce the two types of GO to give the samples summarized in Table 1:

a) Chemical reduction: 10 g of Ascorbic Acid were added to 60 mL of 0.5 mg.mL-1 of GO from Hummers and Tour methods (rGO-AA-H and rGO-AA-T) aqueous dispersion and continuous stirring was applied. After the 48 h reaction time was completed at room temperature, the suspension color has changed from light brown to black while the solid product agglomerates indicating hydrophobicity. Samples were filtered through 0.45 µm cellulose filter, washed with 100 mL of 1M HCl and then with ultrapure water until pH 5.5 - 6 value. Finally, the obtained rGO were dried under vacuum at 80 ˚C for 3 days and ground in an agate mortar.

b) Solvothermal-chemical reduction: 30 mL of the homogeneous dispersions from Hummers and Tour methods (rGO-ST-AA-H and rGO-ST-AA-T) were transferred into 50 mL PTFE-lined vessels and sealed in a stainless steel autoclave to perform a hydrothermal treatment at 120 ºC for 48 h. The resultant material, consisting on a black and agglomerated solid, was transferred to 80 mL

centrifuge tubes, washed with ultrapure water and centrifuged at 9000 rpm for 1h. This process was repeated 3 times. Remaining solid rGO was transferred to a beaker and 60 mL of ultrapure water were added. Then, chemical reduction was performed as is described in the previous paragraph. Finally, remaining solids were washed 3 times by transferring to centrifuge tubes, filling with ultrapure water and centrifuging at 9000 rpm for 1h. The final solid was dried under vacuum at 60 ºC for 24 h, and ground in an agate mortar.

c) Solvothermal-chemical-thermal reduction: In order to increase the reduction degree, several portions of rGO from solvolthermal-chemical reduction were subjected to a final thermal treatment at different temperatures (250, 400 and 600 ºC). rGO was introduced in a furnace and heated at 5ºC.min^{-1} under inert atmosphere (Argon) for 24 h. Resultant rGO samples (rGO-ST-AA-250-H, rGO-ST-AA-250-T, rGO-ST-AA-400-H, rGO-ST-AA-400-T, rGO-ST-AA-600-H and rGO-ST-AA-600-T) were ground in an agate mortar.

Table 1. As-prepared materials and the preparation method.

Samples	Treatments		
	Chemical reduction	**Solvothermal reduction**	**Thermal reduction**
rGO-AA-H	Ascorbic acid, 48 h, RT	-	-
rGO-AA-T	Ascorbic acid, 48 h, RT	-	-
rGO-ST-AA-H	Ascorbic acid, 48 h, RT	48 h, 120 ºC	-
rGO-ST-AA-T	Ascorbic acid, 48 h, RT	48 h, 120 ºC	-
rGO-ST-AA-250-H	Ascorbic acid, 48 h, RT	48 h, 120 ºC	250ºC, 24h, 5ºC.min^{-1}
rGO-ST-AA-250-T	Ascorbic acid, 48 h, RT	48 h, 120 ºC	250ºC, 24h, 5ºC.min^{-1}
rGO-ST-AA-400-H	Ascorbic acid, 48 h, RT	48 h, 120 ºC	400ºC, 24h, 5ºC.min^{-1}
rGO-ST-AA-400-T	Ascorbic acid, 48 h, RT	48 h, 120 ºC	400ºC, 24h, 5ºC.min^{-1}
rGO-ST-AA-600-H	Ascorbic acid, 48 h, RT	48 h, 120 ºC	600ºC, 24h, 5ºC.min^{-1}
rGO-ST-AA-600-T	Ascorbic acid, 48 h, RT	48 h, 120 ºC	600ºC, 24h, 5ºC.min^{-1}

H: GO from Hummers method; T: GO from Tour method; AA: Chemical reduction with ascorbic acid; ST: Solvothermal reduction; 250, 400, 600: Calcination temperature (ºC)

Elemental and structural characterization

X-ray photoelectron spectroscopy (XPS). XPS analysis was performed with a Perkin-Elmer PHI 5400 spectrometer equipped with a Mg Kα excitation source (hν = 1253.6 eV) and a beam size of 1 mm diameter. The spectrometer was calibrated using copper, gold and silver standards. Typical operation conditions were: x-ray gun, 15 kV, 20 mA; pressure in the sample chamber ~ 10-9 Torr; pass energy, 89.50 eV for general spectra (0-1100 eV) and 35.75 eV for high resolution spectra.

Elemental analysis. A LECO TruSpec CHN elemental analyzer was used for the carbon, hydrogen and nitrogen determinations in graphene samples. C and N contents were determined by heating to temperature of at least 900 ºC in the presence of oxygen gas. Mineral and organic compounds were oxidized and/or volatilized to carbon dioxide (CO_2), water (H_2O), nitrogen oxides (NO_x) and molecular nitrogen (N_2). After transforming all nitrogen forms into N_2, the content of total nitrogen was measured using thermal conductivity. The amount of carbon dioxide and water was measured by an infrared detection method.

X-ray Diffraction (XRD). XRD technique was employed to determine crystalline composition. Diffraction data were collected by using a PANalytical X´Pert Pro diffractometer operating in θ-θ configuration, with CuKα radiation (45 kV-40 mA), in the angular range of $5° < 2\theta < 80°$ with a 0.017° step size.

Raman spectroscopy. Raman spectra were acquired by using B&WTek i-RamanTM spectrometer ExemplarPro model, with a green laser HeNe with a wavelength of 532 nm and an operation power of 100 mW. The spectral range available is from 65 - 4000 cm-1, with a pixel resolution of 2.99 cm-1. Raman spectra were acquired with a typical exposition time of ~ 60 s, and 5 accumulations and all acquired spectra were recalibrated using a Neon emission light.

Brunauer-Emmett-teller (BET) analysis. Brunauer-Emmett-teller (BET) method via N_2 absorption-desorption measurements was applied to the as-prepared materials to evaluate the specific surface area of graphene samples using with an ASAP 2020 (Micromeritics). This instrumentation was also employed to evaluate the pores volume of each sample were evaluated.

Results and Discussion

XPS and elemental analysis. Figure 1 presents XPS C1s spectra for each as-prepared material.

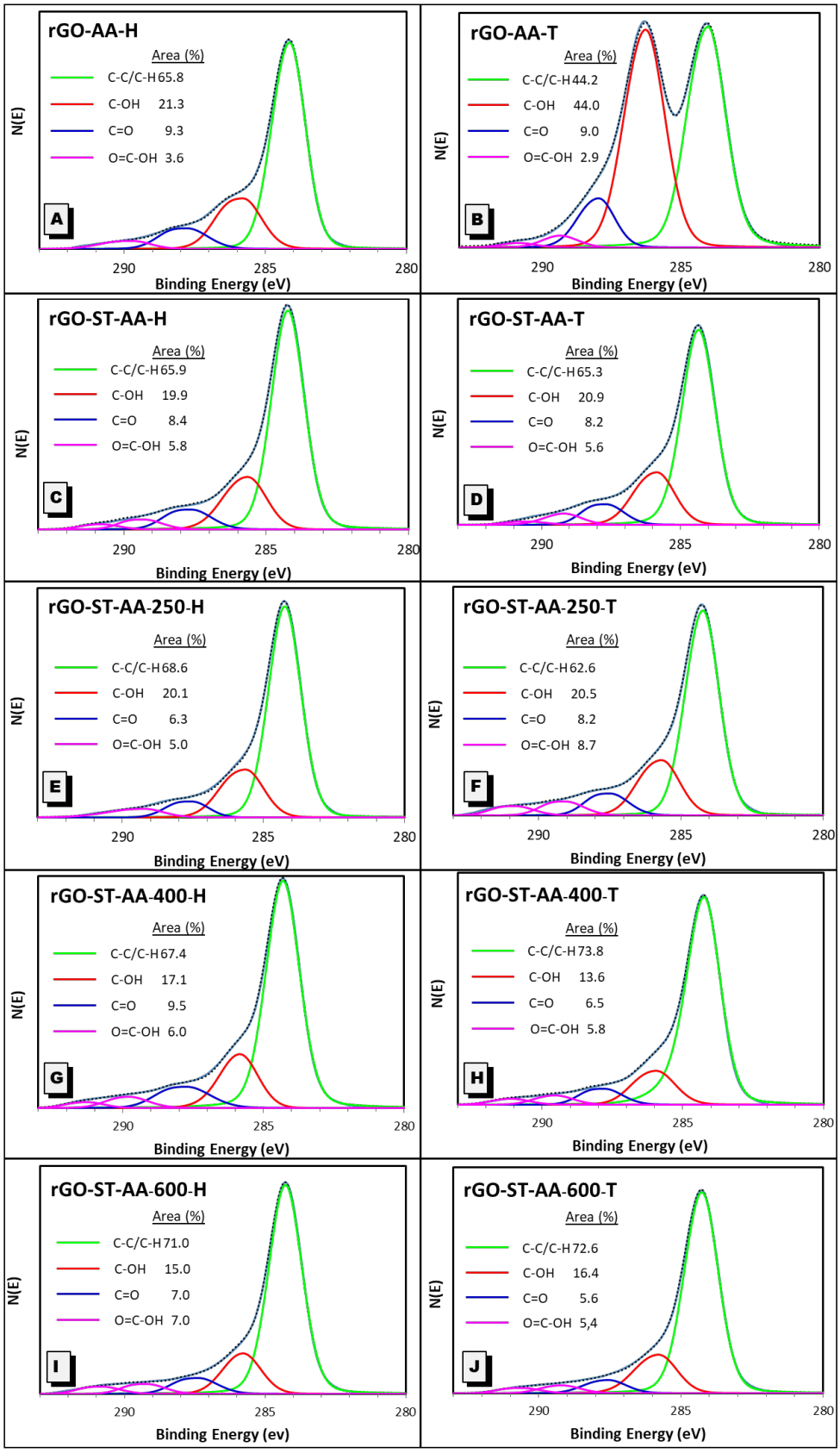

Figure 1. XPS C1s spectra for as-prepared materials. A) rGO-AA-H, B) rGO-AA-T, C) rGO-ST-AA-H, D) rGO-ST-AA-T, E) rGO-ST-AA-250-H, F) rGO-ST-AA-250-T, G) rGO-ST-AA-400-H, H) rGO-ST-AA-400-T, I) rGO-ST-AA-600-H and J) rGO-ST-AA-600-T.

The intensity of peaks corresponding to C=O, located at about 287.5 eV (peak 3), and C-OH (around 285.8 eV, peak 2) decreases more or less gradually with the application of more energetic treatments. Application of solvothermal treatment as well as increasing annealing temperature enhances the effectiveness in removing oxygen groups which results in decreasing of intensities of the bands corresponding to the carboxyl, hydroxyl, or other oxygen functional groups [28,29]. Besides, the peak corresponding to the C-C / C-H (located around 284.2 eV, peak 1) increases as function of reduction steps introduced and, also, increasing temperature in the thermal reduction process. This behaviour is expected since it has been observed in similar studies . The intensities were estimated by calculating the area under each peak after smoothing and removing the background using the modified method of Shirley and adjusting the experimental curve to a Gaussian-Lorentzian ratio variable curve using an iterative algorithm. Results are shown in Table 2.

Table 2. Area percentage of functional groups of the rGO samples.

Sample	Assignation				Ratio
	C-C/C-H	C-OH	C=O	O=C-OH	
	Area % (Position)	Area % (Position)	Area % (Position)	Area % (Position)	C/O
rGO-AA-H	65.8 (284.15)	21.3 (285.80)	9.3 (287.77)	3.6 (289.70)	6.3
rGO-AA-T	44.2 (284.04)	44.0 (286.29)	9.0 (287.98)	2.9 (289.37)	2.5
rGO-ST-AA-H	65.9 (284.24)	19.9 (285.66)	8.4 (287.62)	5.8 (289.28)	6.4
rGO-ST-AA-T	65.3 (284.35)	20.9 (285.85)	8.2 (287.67)	5.6 (289.20)	5.5
rGO-ST-AA-250-H	68.6 (284.25)	20.1 (285.64)	6.3 (287.54)	5.0 (289.22)	6.9
rGO-ST-AA-250-T	62.6 (284.23)	20.5 (285.68)	8.2 (287.48)	8.7 (289.05)	6.1
rGO-ST-AA-400-H	67.4 (284.30)	17.1 (285.84)	9.5 (287.72)	6.0 (289.78)	6.7
rGO-ST-AA-400-T	73.8 (284.25)	13.8 (285.95)	6.5 (287.79)	5.8 (289.54)	7.9
rGO-ST-AA-600-H	71.0 (284.28)	15.0 (285.79)	7.0 (287.37)	7.0 (289.20)	15.9
rGO-ST-AA-600-T	72.6 (284.27)	16.4 (285.79)	5.6 (287.56)	5.4 (289.20)	11.8

The surface atomic percentages of each material were calculated by XPS and C/O atomic ratios are summarized in Table 2. C/O atomic ratios have considerably increased, as a consequence of the oxygen percentage decrease, for rGO-ST-AA-600-H and rGO-ST-AA-600-T (C/O ratio = 15.9 and 11.8), when compared with the C/O atomic ratios of the other samples (C/O ratios between 2.5 and 7.9). In the case of rGO-AA-T, the XPS results confirmed the occurrence of a milder reduction since the decrease of C/O ratio is less pronounced (C/O ratio = 2.5). For comparison, C/O atomic ratios of reduced graphene oxides prepared by the Hummers method are in the range of 6.3–15.9 while C/O atomic ratios of reduced graphene oxides prepared by the Tour method are in the range of 2.5–11.8 which means that a better reduction has been produced with the Hummers method, mainly when reduction is performed by a single chemical procedure. Obtained C/O for rGO-AA-H (6.3) and rGO-AA-T (2.5) are in the same order, but lower, to similar rGOs from the literature (8.0 and 4.4 respectively) [20,30]. The relatively low C/O ratios observed for rGO-AA-H and rGO-AA-T are explained because ascorbic acid reduce epoxy and hydroxyl groups that are located at the basal planes while carbonyl and carboxyl groups, located at the edges of GO structure, occur in a minor extent [15]. According to N. Morimoto et al. [10], GO containing a low quantity of carboxyl and carbonyl groups, that means less oxidized, will be suitable to produce highly conductive and defect-free graphene-like materials via reduction. The application of thermal annealing in the range of 200-900 ºC cause the progressive decarboxylation although carbonyl groups remain [31].

Moreover, the extent reduction of each sample has been also estimated performing elemental analysis. Figure 2 shows the obtained results. As it can be observed the carbon percentage increases

with the application of reduction treatments. So, applying only chemical treatment, carbon percentages are 59 % and 76 % for rGO-AA-T and rGO-AA-H respectively, while the combinations of solvothermal, chemical and thermal (600 ºC) achieve carbon percentages of 85 % and 82 % for rGO-ST-AA-600-H and rGO-ST-AA-600-T respectively. Regarding Tour method is evident that the combination of reduction methods increases the percentage of carbon and therefore the degree of reduction. In the case of applying thermal treatment, higher temperature produces higher percentage of carbon, this effect is also observed in samples with modified Hummers method applied [10].

These results confirm the XPS obtained results. The percentage of carbon is higher in samples oxidized with Hummers method, probably caused by a lower extent of oxidation for these samples. Nevertheless, samples obtained applying Tour method present a lower percentage of carbon, which could be due to a more energetic oxidation process.

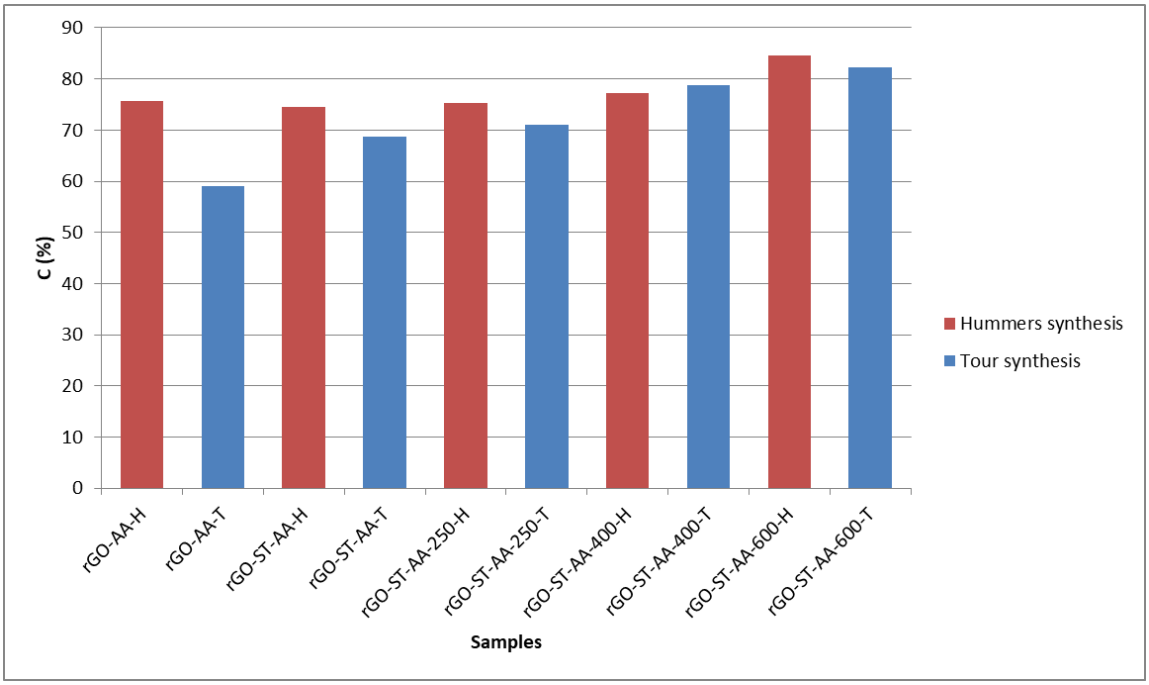

Figure 2. Carbon concentrations in each sample expressed as atomic percentage.

X-ray diffraction. XRD patterns of the rGO samples as a function of reductions methods applied are presented in Figure 3. Figure 3a shows two XRD profiles very different. rGO-AA-T present the highest peak at 11.48° (2Θ) (table 3), which correspond to [0 0 1] GO peak without to be reduced to rGO. In spite of the low crystallinity of rGO materials, rGO-AA-H presents a peak at 23.10° (2Θ) (table 3) that is near to [0 0 2] graphite peak, 2Θ=26.43º (PDF # 00-008-0415), due to the tendency of the reduced materials to recovery the original graphite structure [27].

After applying solvothermal and chemical treatment and also after applying thermal treatment to 250° C the XRD patterns obtained present similar tendency (figure 3b and 3c, respectively). The principal peak, table 3, is more displaced towards [0 0 2] graphite peak, 2Θ=26.43º. Thermal reduction promotes to remove the most labile oxygen groups, many of which are attacked with great efficacy using a step of chemical reduction [27], which means, that thermal expansion, to 250° C, do not practically contribute to reduce the material.

XRD patterns of rGO-ST-AA-400 and rGO-ST-AA-600 samples are very similar (figure 3d and 3e). As it is shows in table 3, the position of the principal peak is quite similar in the four samples and nearest to that of graphite [0 0 2] peak, indicating a higher reduction power of these multiphase reduction methods.

Near to 2Θ= 43º [1 0 0] graphene diffraction peaks appear, indicating a short-range order in stacked graphene layers.

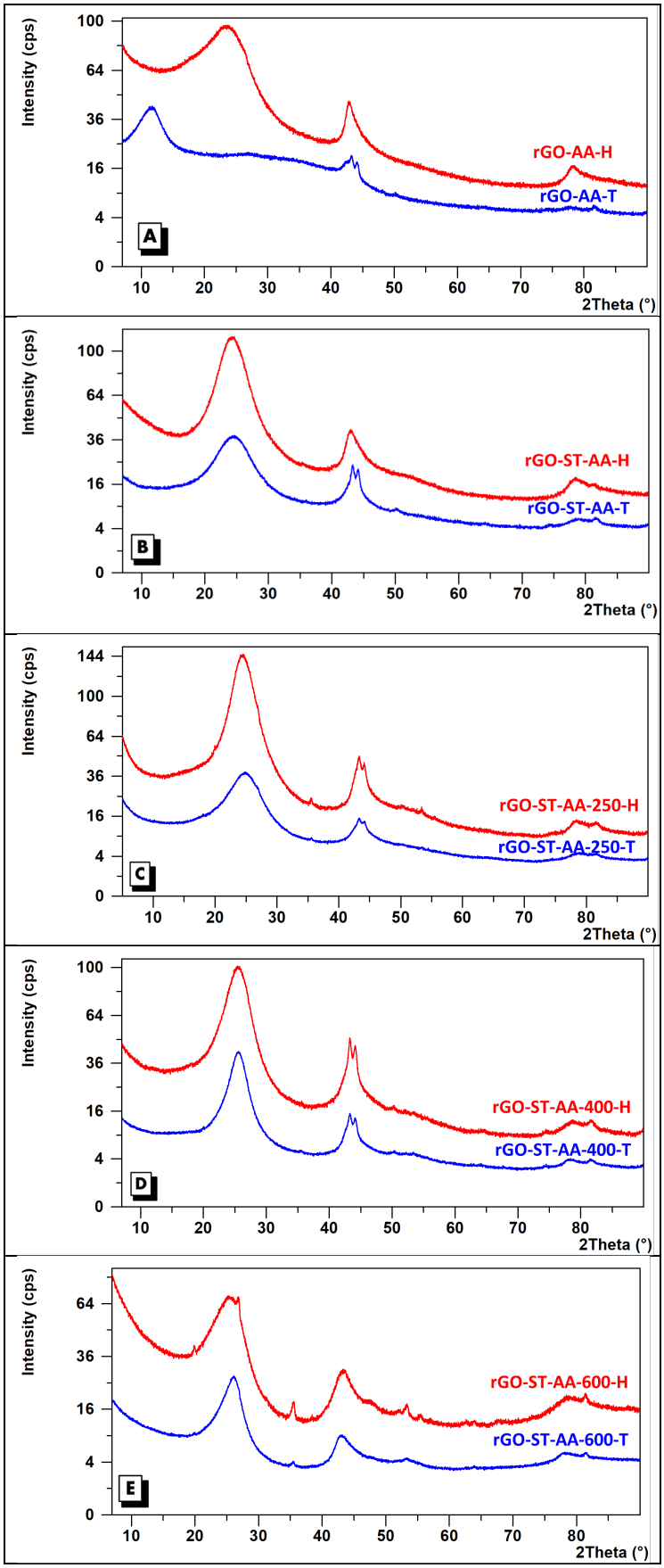

Figure 3. XRD patterns of the rGO synthetized samples. A) rGO-AA-H and rGO-AA-T, B) rGO-ST-AA-H and rGO-ST-AA-T, C) rGO-ST-AA-250-H and rGO-ST-250-AA-T, D) rGO-ST-AA-400-H and rGO-ST-400-AA-T and E) rGO-ST-AA-600-H and rGO-ST-600-AA-T.

The sample rGO-ST-AA-600-H presents the peak nearest to graphite [0 0 2] peak. This result is agreed with XPS results, because this is the sample with highest carbon percentage (figure 2). In both analyses, rGO-ST-AA-600-H sample largely eliminated the oxygen groups.

Table 3. XRD peaks at different angles and crystallite size (L).

Sample	GO peak position (2Θ)	rGO peak position (2Θ)	L (nm)
rGO-AA-H	-	23.10	4.42
rGO-AA-T	11.48	-	8.45
rGO-ST-AA-H	-	24.40	5.63
rGO-ST-AA-T	-	24.53	4.99
rGO-ST-AA-250-H	-	24.47	6.62
rGO-ST-AA-250-T	--	24.64	5.25
rGO-ST-AA-400-H	--	25.29	6.46
rGO-ST-AA-400-T	-	25.43	9.30
rGO-ST-AA-600-H	-	25.61	8.84
rGO-ST-AA-600-T	-	25.12	6.20

The crystalline size (L) of the as-prepared materials were calculated applying the following equation [32] (1).

$$L = \frac{1.84 * \lambda}{\beta * \cos\theta} \quad (1)$$

Where β = full width at half maximum (FWHM) at the diffraction angle 2Θ, λ=X-ray wavelength.

The estimated size from the XRD analysis is shown in table 3. The crystallinity of the as-prepared materials in Hummers synthesis increases with increase in treatments and temperature. In Tour method these effects are not so clear and rGO-ST-AA-600-T present a crystallite size smaller than rGO-AA-T.

Raman spectroscopy can be used for quantifying the extent of the sp^3 to sp^2 transformation. The typical Raman spectra of rGO is composed by two strong bands located at ~1350 cm^{-1} and ~1590 cm^{-1}, assigned to D- and G-band respectively, and an broad band at 2750-3000 cm-1 correspondind to the overtone 2D-band [33,34]. On the one hand, the intensity ratio of the D and G bands (I_D/I_G) reflects the defect density, thus, the I_D/I_G ratio is larger when the surface has more defects. On the other hand, as the ratio I_{2D}/I_G increases the reduction increases [35,36]. Figure 4 shows the spectra obtained after each treatment. Each spectrum depicted in this figure corresponds to an average spectrum of the three ones acquired at different points on the surface, which were similar, thus confirming the homogeneity of the samples. Then, all spectra were normalized with the G-band intensity.

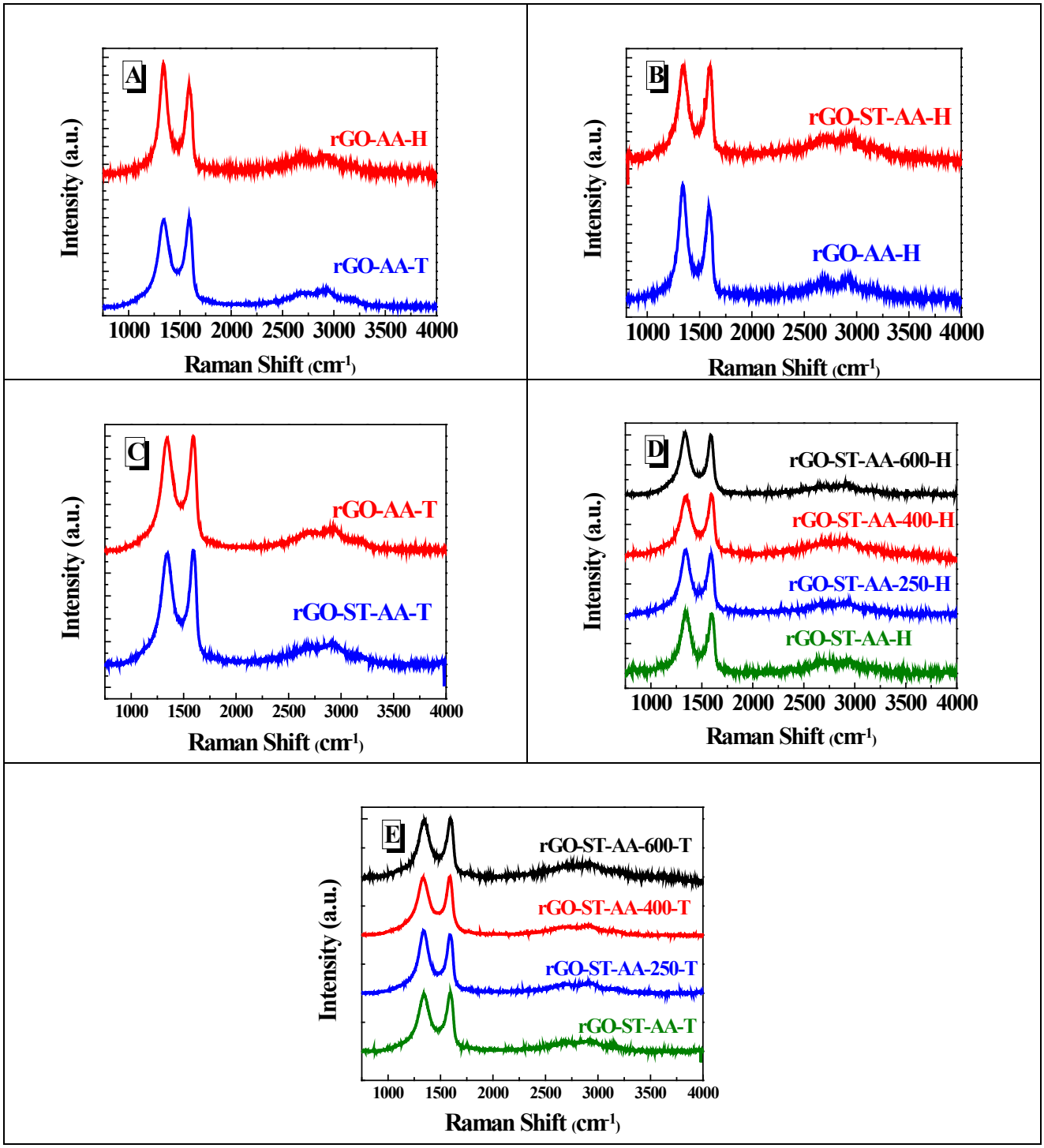

Figure 4. Evolution of Raman spectra at the different reduction methods. Each spectrum corresponds to an average spectrum of the three spectra acquired at different points on the surface. Note that all spectra were normalized with the G-band intensity. A) A) rGO-AA-H and rGO-AA-T, B) rGO-AA-H and rGO-ST-AA-H, C) rGO-AA-T and rGO-ST-AA-T, D) rGO-ST-AA-H, rGO-ST-AA-250-H, rGO-ST-AA-400-H and rGO-ST-600-AA-H and E) rGO-ST-AA-T, rGO-ST-AA-250-T, rGO-ST-AA-400-T and rGO-ST-600-AA-T.

Figure 4.A. illustrates the comparison of the chemical reduction of GO obtained by modified Hummers method (rGO-AA-H) and Tour method (rGO-AA-T). As it can be seen, there is a slight increase in the 2D-band for the rGO-AA-T sample, which suggests that more sp^2 domains are formed for samples from the Hummers method than those obtained from the Tour method. Moreover, the D-band is higher in the rGO-AA-T, indicating more defects for samples from the Tour method.

Figure 4.B. and 4.C. point out the effect of the solvothermal reduction on the two methods (Hummers and Tour, respectively). Thus, in the Tour method the effect of the solvothermal reduction it is not appreciable, (spectra shown in Figure 4.C are very similar). On the contrary, it can be noticed the reduction of the defects in the Hummers methods after the solvothermal reduction (decrease in the D band corresponding to the rGO-ST-AA-H).

Figure 4.D and Figure 4.E show the Raman spectra obtained after thermal reduction performed at different temperatures, for the Hummers and Tour methods respectively. In this comparison no appreciable variation can be found.All rGO as-prepared materials exhibited intense G band and D bands, confirming the existence of defects in the layers of graphene. The calcutated corresponding I_D/I_G ratio values ranged between 1.00 and 1.20 in all samples, which are similar to those found by other authors [32].

Table 4. Textural properties of the as-prepared materials.

Sample	SSA ($m^2.g^{-1}$)	Pore Volume ($cm^3.g^{-1}$)
rGO-AA-H	429	0.38
rGO-AA-T	233	0.13
rGO-ST-AA-H	152	0.11
rGO-ST-AA-T	403	0.24
rGO-ST-AA-250-H	194	0.13
rGO-ST-AA-250-T	142	0.084
rGO-ST-AA-400-H	404	0.34
rGO-ST-AA-400-T	678	0.53
rGO-ST-AA-600-H	476	0.40
rGO-ST-AA-600-T	827	0.52

Brunauer-Emmett-teller (BET) analysis. Table 4 exhibits the textural properties of the as-prepared materials. The SSA (specific surface area) and pore volume, in general, are higher in samples with Tour oxidation method. This oxidation method presents some modifications to the modified Hummers oxidation method such as using high concentration of $KMnO_4$ and using excess of H_2SO_4 and H_3PO_4 without using $NaNO_3$. This modification helped to avoid the production of toxic NO_2 and N_2O_4 and increase product yield and GO formed present water groups intercalated between graphite sheets [37], while modified Hummers method products materials with high extent of oxidation, corroborated by XPS and elemental analysis.

Differences, SSA and pore volume, between modified Hummers method and Tour method are more visible in rGO samples with final thermal treatment which can be due to the expansion of graphene sheets in the reduction process by the water groups intercalated between graphite sheets. This effect is more visible in rGO samples with the three treatments where the combinations of treatments advantage this effect.

Conclusions

In this work, the feasibility of GO obtained by both Hummers and Tour method to prepare rGO as well as chemically reduction using a green reductant under different experimental conditions were evaluated with a view to their possible applications, which are a function of the reduction degree and the abundance and types of oxygen functional groups.

Characterization analysis showed a higher oxidation degree for samples from Tour method than those oxidized by Hummers method. This suggests the suitability of Tour graphene oxide (GO-T) for chemical functionalization which is very useful for several applications. On the contrary, lower oxidation degree from Hummers graphene oxide (GO-H) may facilitate the subsequent reduction process leading to a higher reduced rGO. Hence, rGO samples obtained from the Hummers method in the different reduction treatments presented higher C/O atomic ratios than the corresponding

Tour method. In addition, the combination of the solvothermal treatment and chemical reduction, and more importantly, including a final annealing stage, increases significantly the value of the C/O ratio and therefore GO reduction is markedly improved. Besides, XPS and Raman analysis demonstrated that annealing treatment contributes to decrease the defect density and the restoration of π-conjugated structure.

In general, rGO samples obtained from Tour method presented higher SSA and pore volume than those samples obtained from Hummers method, indicating that both GO and rGO coming from Tour method are more appropriate to applications in which high surface area is required.

The present paper underscores the key items that should be considered when performing the synthesis of GO and rGO, which can be supportive to select the most feasible methodology to synthesize GO and rGO materials depending on the future application. Taking into account that the highest C/O ratios have been obtained after three consecutive reduction stages future studies should be focused on optimising the methodology for obtaining highly reduced rGO by a fewer reducing steps.

Funding Sources

Financial support DIGRAFEN (Grant ENE2017-88065-C2-2-R funded by MCIN/AEI/ 10.13039/501100011033 and by ERDF A way of making Europe) and REGRAP-2D (Grant PID2020-114234RB-C21 funded by MCIN/AEI/ 10.13039/501100011033) the XRD equipment CIEM05-34-03 from FEDER 2004.

Abbreviations

BET, Brunauer-Emmett-teller analysis, GO, graphene oxide; GrO, graphite oxide; rGO, reduced graphene oxide; SSA, specific surface area; XPS, X-ray photoelectron spectroscopy; XRD. X-ray diffraction.

References

[1]. M. J. Allen, V. C. Tung, R. B. Kaner, Honeycomb Carbon: A Review of Graphene, Chemical Reviews 110 (1) (2010) 132-145.

[2]. A. K. Geim, K. S. Novoselov, The rise of graphene, Nat. Mater. 6 (3) (2007) 183-191.

[3]. K. S. Novoselov, A. K. Geim, S. V. Morozov, D. Jiang, Y. Zhang, S. V. Dubonos, I. V. Grigorieva, A. A. Firsov, Electric field effect in atomically thin carbon films, Science 306 (5696) (2004) 666-669.

[4]. C. Zhu, S. Guo, Y. Fang, S. Dong, Reducing Sugar: New Functional Molecules for the Green Synthesis of Graphene Nanosheets, ACS Nano 4 (4) (2010) 2429-2437.

[5]. B. F. Machado, P. Serp, Graphene-based materials for catalysis, Catalysis Science & Technology 2 (1) (2012) 54-75.

[6]. V. B. Mohan, K.-T. Lau, D. Hui, D. Bhattacharyya, Graphene-based materials and their composites: A review on production, applications and product limitations, Composites Part B: Engineering 142 ((2018) 200-220.

[7]. A. G. Olabi, M. A. Abdelkareem, T. Wilberforce, E. T. Sayed, Application of graphene in energy storage device – A review, Renewable and Sustainable Energy Reviews 135 (C) (2021) S1364032120303178.

[8]. A. K. Sood, I. Lund, Y. R. Puri, H. Efstathiadis, P. Haldar, N. K. Dhar, J. Lewis, M. Dubey, E. Zakar, P. Wijewarnasuriya, Review of graphene technology and its applications for electronic devices, Graphene—New Trends and Developments (2015).

[9]. A. Malas Rubber nanocomposites with graphene as the nanofiller. In, 2017.

[10]. N. Morimoto, T. Kubo, Y. Nishina, Tailoring the Oxygen Content of Graphite and Reduced Graphene Oxide for Specific Applications, Scientific Reports 6 (1) (2016) 21715.

[11]. W. S. Hummers, R. E. Offeman, PREPARATION OF GRAPHITIC OXIDE, J. Am. Chem. Soc. 80 (6) (1958) 1339-1339.

[12]. S. Stankovich, D. A. Dikin, G. H. B. Dommett, K. M. Kohlhaas, E. J. Zimney, E. A. Stach, R. D. Piner, S. T. Nguyen, R. S. Ruoff, Graphene-based composite materials, Nature 442 (7100) (2006) 282-286.

[13]. D. C. Marcano, D. V. Kosynkin, J. M. Berlin, A. Sinitskii, Z. Z. Sun, A. Slesarev, L. B. Alemany, W. Lu, J. M. Tour, Improved Synthesis of Graphene Oxide, ACS Nano 4 (8) (2010) 4806-4814.

[14]. K. Erickson, R. Erni, Z. Lee, N. Alem, W. Gannett, A. Zettl, Determination of the Local Chemical Structure of Graphene Oxide and Reduced Graphene Oxide, Advanced Materials 22 (40) (2010) 4467-4472.

[15]. K. K. H. De Silva, H.-H. Huang, M. Yoshimura, Progress of reduction of graphene oxide by ascorbic acid, Applied Surface Science 447 ((2018) 338-346.

[16]. M. Kaur, K. Pal, An investigation for hydrogen storage capability of zirconia-reduced graphene oxide nanocomposite, International Journal of Hydrogen Energy 41 (47) (2016) 21861-21869.

[17]. R. S. Rajaura, S. Srivastava, V. Sharma, P. K. Sharma, C. Lal, M. Singh, H. S. Palsania, Y. K. Vijay, Role of interlayer spacing and functional group on the hydrogen storage properties of graphene oxide and reduced graphene oxide, International Journal of Hydrogen Energy 41 (22) (2016) 9454-9461.

[18]. X. Zhang, K. Li, H. Li, J. Lu, Q. Fu, Y. Chu, Graphene nanosheets synthesis via chemical reduction of graphene oxide using sodium acetate trihydrate solution, Synthetic Metals 193 ((2014) 132-138.

[19]. F. Cataldo, O. Ursini, G. Angelini, Graphite Oxide and Graphene Nanoribbons Reduction with Hydrogen Iodide, Fullerenes, Nanotubes and Carbon Nanostructures 19 (5) (2011) 461-468.

[20]. S. Abdolhosseinzadeh, H. Asgharzadeh, H. Seop Kim, Fast and fully-scalable synthesis of reduced graphene oxide, Scientific Reports 5 (1) (2015) 10160.

[21]. M. J. Fernández-Merino, L. Guardia, J. I. Paredes, S. Villar-Rodil, P. Solís Fernández, A. Martínez-Alonso, J. TascóN, Vitamin C Is an Ideal Substitute for Hydrazine in the Reduction of Graphene Oxide Suspensions, Journal of Physical Chemistry C - J PHYS CHEM C 114 ((2010) 6426-6432.

[22]. C.-Y. Ho, H.-W. Wang, Characteristics of thermally reduced graphene oxide and applied for dye-sensitized solar cell counter electrode, Applied Surface Science 357 ((2015) 147-154.

[23]. A. Klechikov, G. Mercier, T. Sharifi, I. A. Baburin, G. Seifert, A. V. Talyzin, Hydrogen storage in high surface area graphene scaffolds, Chemical Communications 51 (83) (2015) 15280-15283.

[24]. A. Ladron-De-Guevara, A. Bosca, J. Pedros, E. Climent-Pascual, A. De Andres, F. Calle, J. Martinez, Reduced graphene oxide/polyaniline electrochemical supercapacitors fabricated by laser, Applied Surface Science 467 ((2019) 691-697.

[25]. C. Nethravathi, M. Rajamathi, Chemically modified graphene sheets produced by the solvothermal reduction of colloidal dispersions of graphite oxide, Carbon 46 ((2008) 1994-1998.

[26]. M. M. M. Alyobi, C. Barnett, R. J. Cobley Effects of Thermal Annealing on the Properties of Mechanically Exfoliated Suspended and On-Substrate Few-Layer Graphene. In, 2017.

[27]. M. P. Lavin-Lopez, A. Paton-Carrero, L. Sanchez-Silva, J. L. Valverde, A. Romero, Influence of the reduction strategy in the synthesis of reduced graphene oxide, Advanced Powder Technology 28 (12) (2017) 3195-3203.

[28]. Y. Ahn, J. Kim, S. Ganorkar, Y.-H. Kim, S.-I. Kim, Thermal annealing of graphene to remove polymer residues, Materials Express 6 (1) (2016) 69-76.

[29]. F. Han, S. Yang, W. Jing, K. Jiang, Z. Jiang, H. Liu, L. Li, Surface plasmon enhanced photoluminescence of ZnO nanorods by capping reduced graphene oxide sheets, Opt. Express 22 (10) (2014) 11436-11445.

[30]. J. Jagiełło, A. Chlanda, M. Baran, M. Gwiazda, L. Lipińska, Synthesis and Characterization of Graphene Oxide and Reduced Graphene Oxide Composites with Inorganic Nanoparticles for Biomedical Applications, Nanomaterials (Basel) 10 (9) (2020) 1846.

[31]. X. Gao, J. Jang, S. Nagase, Hydrazine and Thermal Reduction of Graphene Oxide: Reaction Mechanisms, Product Structures, and Reaction Design, The Journal of Physical Chemistry C 114 (2) (2010) 832-842.

[32]. A. Kaushal, S. K. Dhawan, V. Singh, Determination of crystallite size, number of graphene layers and defect density of graphene oxide (GO) and reduced graphene oxide (RGO), AIP Conference Proceedings 2115 (1) (2019) 030106.

[33]. A. C. Ferrari, D. M. Basko, Raman spectroscopy as a versatile tool for studying the properties of graphene, Nature Nanotechnology 8 (4) (2013) 235-246.

[34]. D. Yang, A. Velamakanni, G. Bozoklu, S. Park, M. Stoller, R. D. Piner, S. Stankovich, I. Jung, D. A. Field, C. A. Ventrice, R. S. Ruoff, Chemical analysis of graphene oxide films after heat and chemical treatments by X-ray photoelectron and Micro-Raman spectroscopy, Carbon 47 (1) (2009) 145-152.

[35]. R. Arul, R. N. Oosterbeek, J. Robertson, G. Xu, J. Jin, M. C. Simpson, The mechanism of direct laser writing of graphene features into graphene oxide films involves photoreduction and thermally assisted structural rearrangement, Carbon 99 ((2016) 423-431.

[36]. D. Lopez-Diaz, M. Lopez Holgado, J. L. Garcia-Fierro, M. Mercedes Velazquez, Evolution of the Raman Spectrum with the Chemical Composition of Graphene Oxide, Journal of Physical Chemistry C 121 (37) (2017) 20489-20497.

[37]. R. Ikram, B. M. Jan, W. Ahmad, An overview of industrial scalable production of graphene oxide and analytical approaches for synthesis and characterization, Journal of Materials Research and Technology 9 (5) (2020) 11587-11610.